

Supplementary Materials for
**CCR2 cooperativity promotes hematopoietic stem cell homing to the
bone marrow**

Stephanie N. Hurwitz *et al.*

Corresponding author: Stephanie N. Hurwitz, sthurw@iu.edu;
Peter Kurre, kurrep@chop.edu

Sci. Adv. **10**, eadq1476 (2024)
DOI: 10.1126/sciadv.adq1476

The PDF file includes:

Figs. S1 to S7
Legend for movie S1
Legends for data S1 to S3

Other Supplementary Material for this manuscript includes the following:

Movie S1
Data S1 to S3

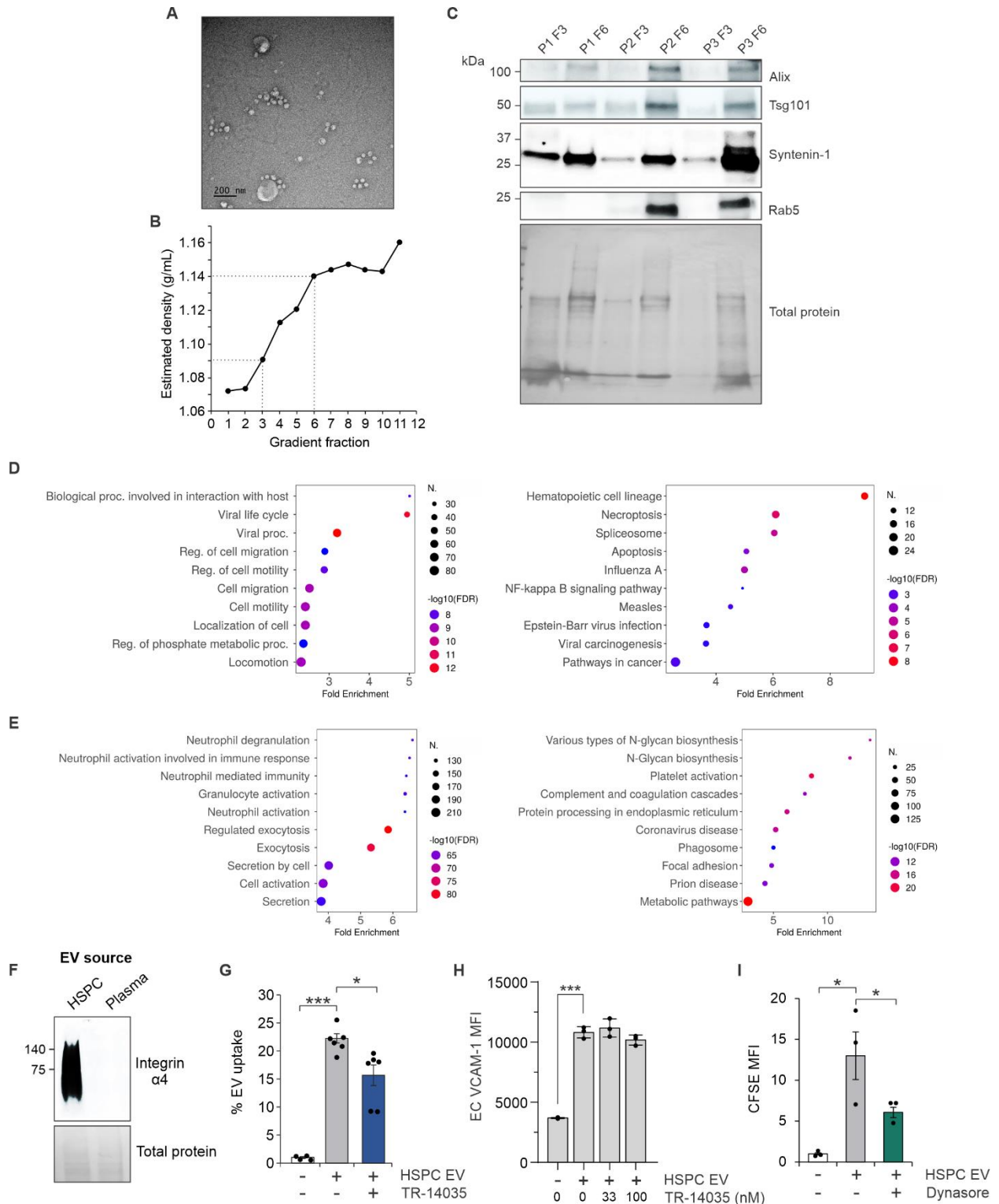


Fig. S1.

Characterization of HSPC and plasma derived EVs from human and murine hematopoietic progenitor cells. A) Representative electron micrograph of isolated EVs. B) Density measurements of fractions in iodixanol gradient used to purify plasma-derived EVs. C)

Representative immunoblots of purified gradient fractions demonstrating enrichment of EV associated proteins in fractions (F3, F6) pooled for mass spectrometry from three donors (P1-3). Gene ontology (left) and KEGG pathway (right) analysis of proteins enriched in **D**) HSPC EVs or **E**) plasma EVs. **F**) Representative immunoblot demonstrating markedly enhanced secretion of integrin $\alpha 4$ in murine HSPC EVs compared to equal numbers of murine plasma EVs. **G**) Flow cytometric measurement of CFSE-dyed EV uptake into ECs. TR-14035, integrin $\alpha 4\beta 1/7$ inhibitor (80 nM). **H**) Flow cytometric levels of median fluorescence intensity (MFI) of VCAM-1 on bone marrow (BM) endothelial cells (EC) after HSPC EV transfer and integrin $\alpha 4\beta$ inhibition using TR-14035. **I**) Flow cytometric measurement of CFSE-dyed HSPC EVs into ECs after dynasore (80 μ M) treatment. *, $p < 0.05$; **, $p < 0.01$; ***, $p < 0.001$.

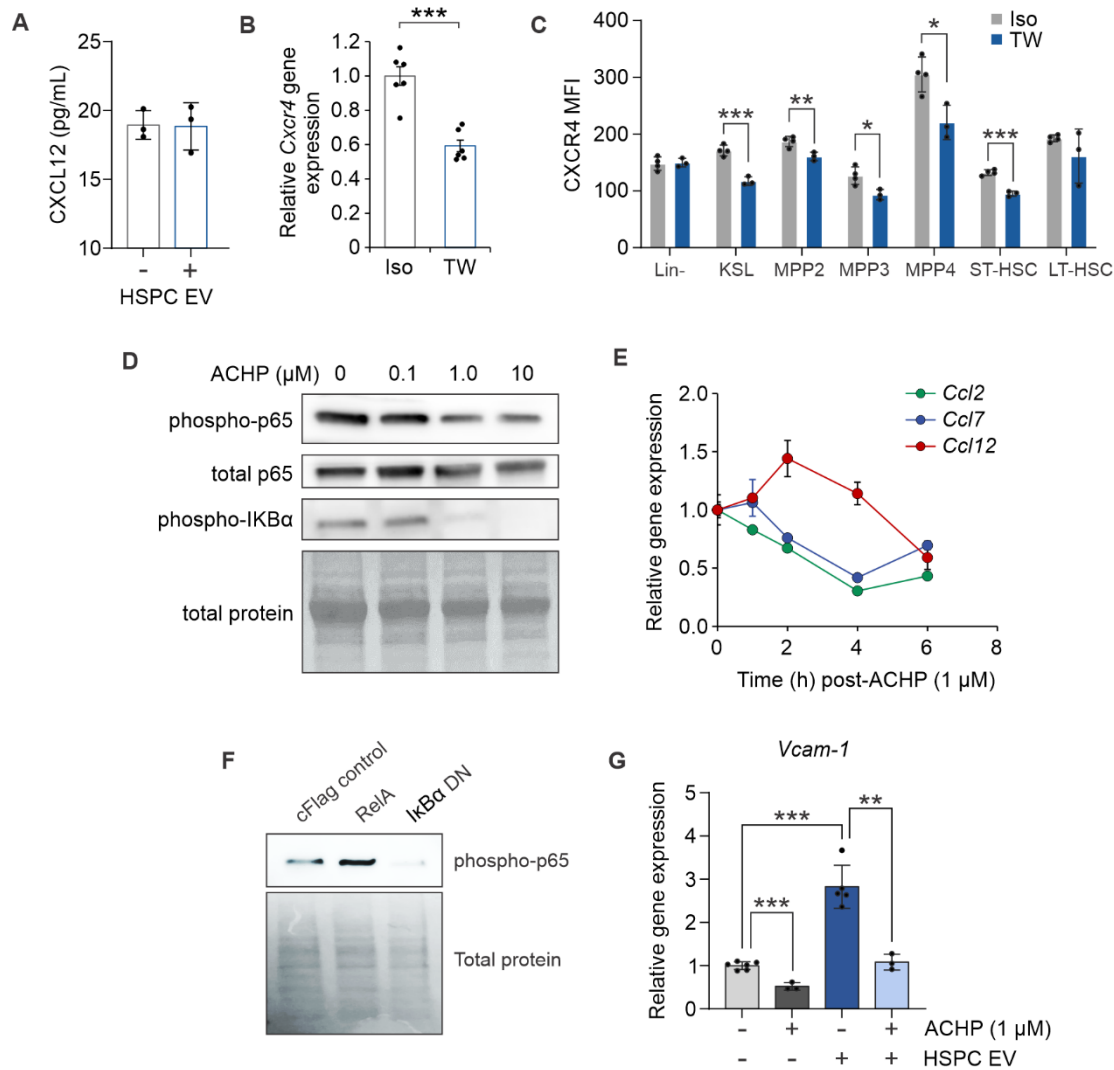


Fig. S2.

HSPC EVs trigger chemokine upregulation in bone marrow endothelial cells. **A)** Enzyme linked immunosorbent assay measuring CXCL12 in endothelial cell (EC) cultures following HSPC EV uptake. **B)** Relative gene expression of *Cxcr4* on HSPCs in EC transwell cultures. **C)** Median intensity fluorescence (MFI) of surface CXCR4 on HSPC subpopulations after EC transwell culture. **D)** Representative immunoblot showing dose-dependent impact of ACHP on NF- κ B inhibition in bone marrow (BM) ECs. **E)** Relative gene expression of CCR2 ligands in ECs after ACHP treatment. **F)** Representative immunoblot showing phosphorylated p65 levels after transduction with the dominant negative I κ B α mutant (RelA overexpression plasmid as a control). **G)** Relative gene expression of *Vcam-1* in ECs after ACHP treatment. Iso, isolated. TW, transwell. *, $p < 0.05$; **, $p < 0.01$; ***, $p < 0.001$.

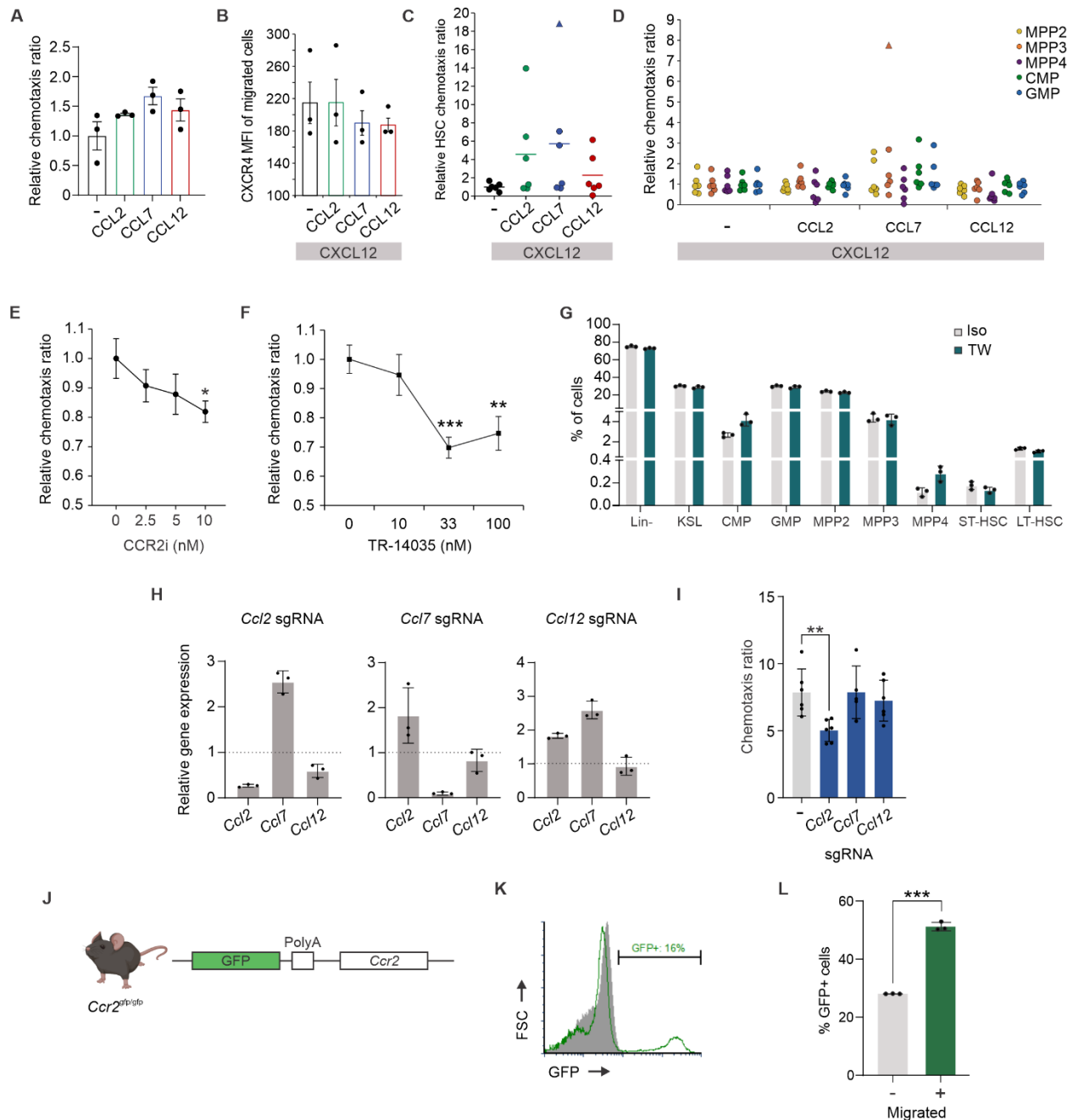


Fig. S3.

HSPC-endothelial cell crosstalk drives chemotaxis via CCR2. **A)** Chemotaxis ratio of murine HSPCs through 5 μ m pores toward CCR2L chemokine gradients in the absence of CXCL12. **B)** Median fluorescence intensity (MFI) of CXCR4 on migrated HSPCs. Chemotaxis ratio of **C)** HSCs or **D)** multipotent progenitors (MPP) and myeloid progenitors (CMP, GMP) toward chemokine gradients. Dose-dependent effect of **E)** CCR2 inhibition (CCR2i) and **F)** integrin $\alpha 4\beta$ inhibition on HSPC chemotaxis. **G)** Relative subpopulation frequency of HSPCs during EC transwell culture. Iso, isolated. TW, transwell. **H)** Relative gene

expression of all CCR2 ligands (CCR2L) in bone marrow (BM) endothelial cells (ECs) after individual gene knockout by CRISPR/Cas9 and HSPC transwell culture, demonstrating compensatory upregulation of residual CCR2L (wild-type EC, dotted line). **I**) Chemotaxis ratio of HSPCs toward ECs harboring individual CCR2 ligand knockouts. **J**) Cassette insert in *Ccr2^{gfp/gfp}* mice; schematic created using BioRender. **K**) Representative flow cytometry plot showing the proportion of GFP⁺ cells in peripheral blood of *Ccr2^{gfp/gfp}* mice. **L**) Proportion of GFP⁺ HSPCs in migrated cell fraction following chemotaxis assay. *, p<0.05; **, p<0.01; ***, p<0.001. Triangle points indicate statistically significant outliers.

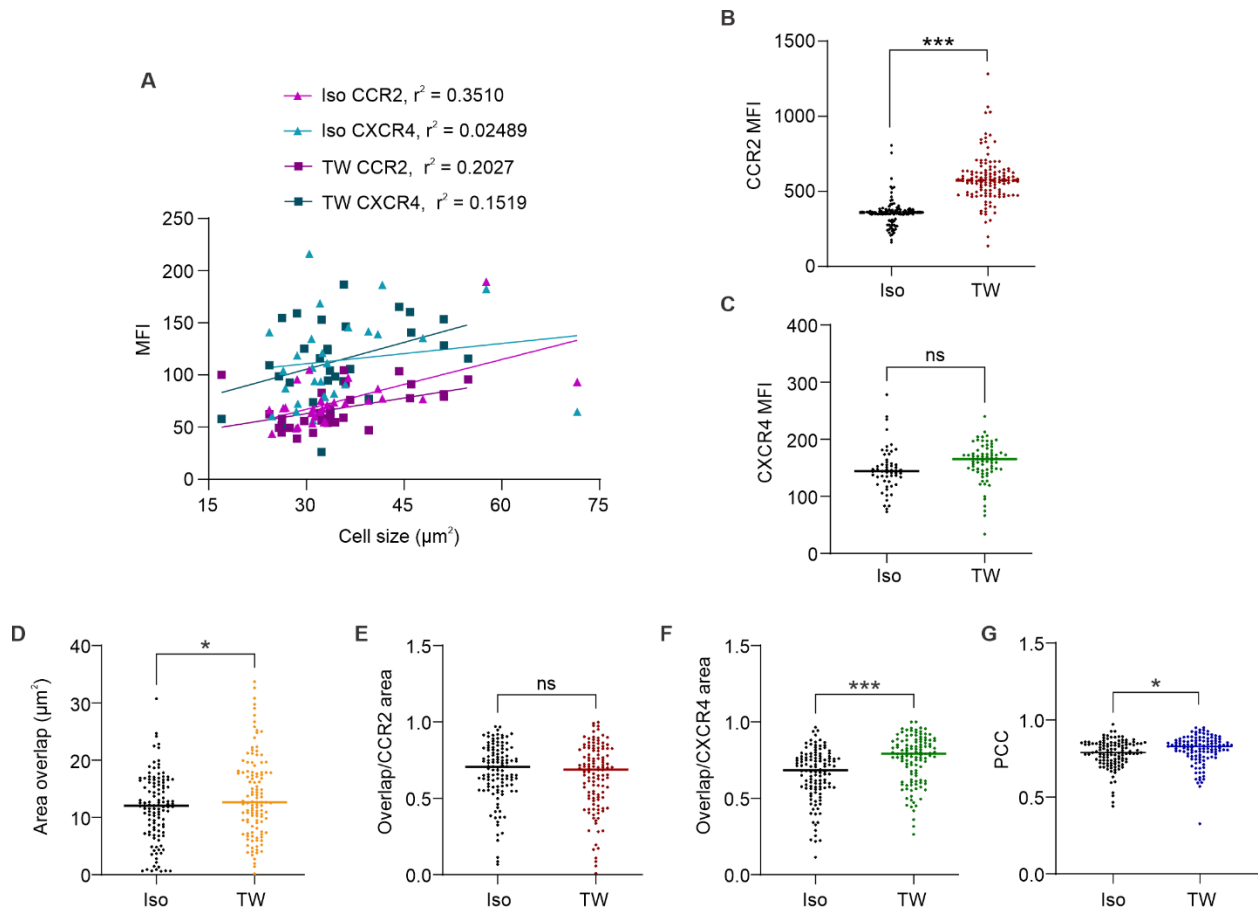


Fig. S4.

EC co-culture drives increased CCR2 and CXCR4 interaction. **A)** Median fluorescence intensity (MFI) of CCR2 and CXCR4 on HSPCs grown in isolation (Iso) or in EC transwell co-culture (TW) plotted against cell size. Quantification of **B)** CCR2 and **C)** CXCR4 MFI per cell ($n=55-126$ cells per condition) in HSPCs cultured in isolation versus EC transwell culture. Measurement of CCR2 and CXCR4 fluorescence **D)** area overlap, **E)** area overlap/CCR2 area, **F)** area overlap/CXCR4 area, and **G)** Pearson correlation coefficient (PCC) in thresholded images ($n= 118-120$ cells per condition). ns, not significant; *, $p<0.05$; ***, $p<0.001$.

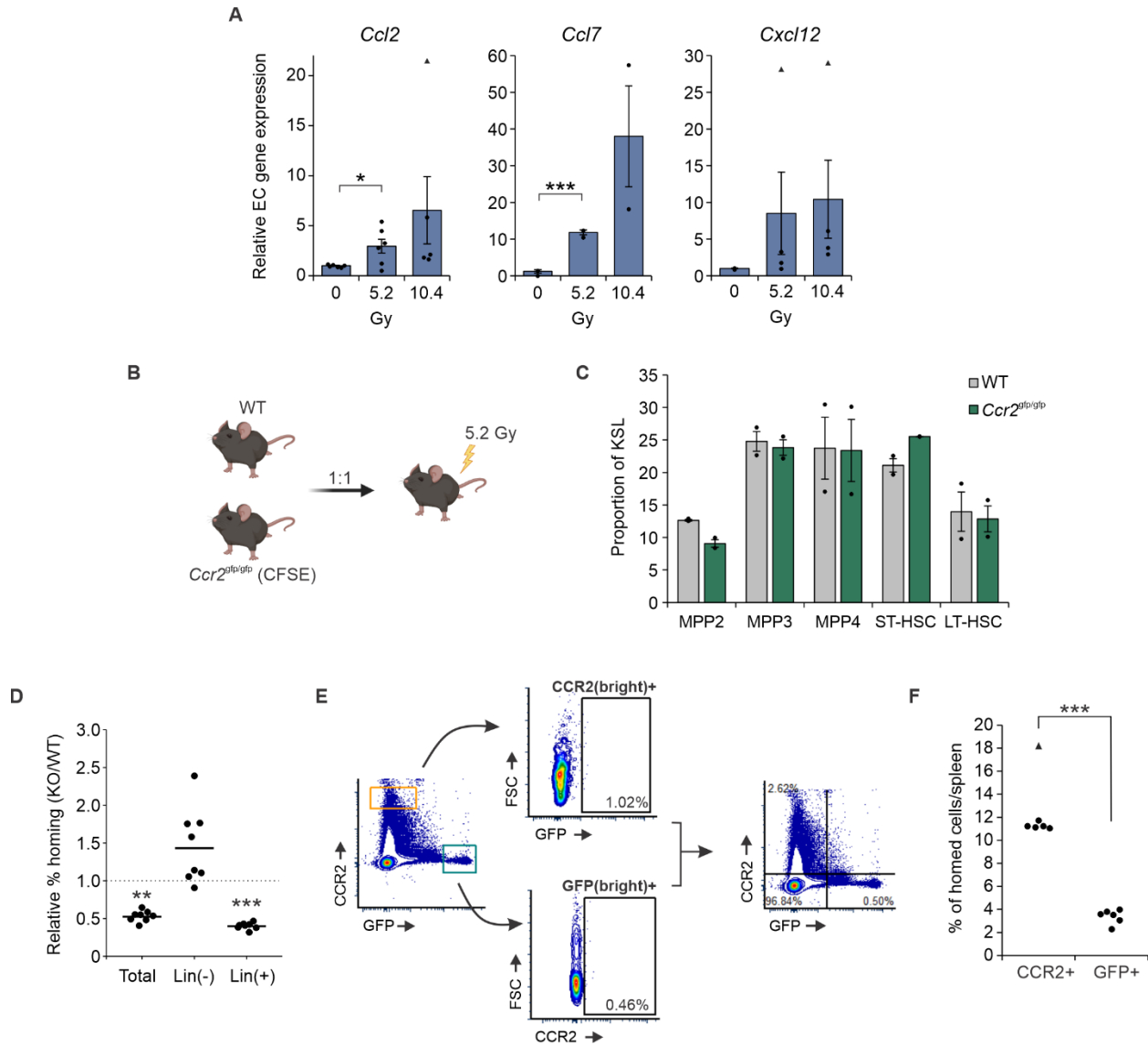


Fig. S5.

Characterization of *Ccr2*^{gfp/gfp} HSPCs at homeostasis and during bone marrow homing. A) Relative chemokine gene expression in wild-type (WT) bone marrow (BM) endothelial cells (ECs) after escalated doses of total body irradiation. **B)** Experimental schematic of competitive transplantations (1:1 donor ratio) using wild-type (WT) and CFSE-dyed *Ccr2*^{gfp/gfp} bone marrow (n=8). Recipient mice were conditioned with a sub-lethal dose (5.2 Gy) of total body irradiation. Created with BioRender. **C)** Relative proportions of HSPC subpopulations in WT versus *Ccr2*^{gfp/gfp} bone marrow. **D)** Flow cytometric analysis of comparative homing between WT and CCR2-deficient grafts 20 hours post-transplantation. **E)** Gating schematic to identify CCR2⁺ versus GFP⁺ cells following competitive transplantation of WT versus *Ccr2*^{gfp/gfp} bone marrow. **F)** Frequency of WT CCR2⁺ and *Ccr2*^{gfp/gfp} GFP⁺ donor cells in the spleen 20 hours post-transplantation. *, p<0.05; **, p<0.01; ***, p<0.001.

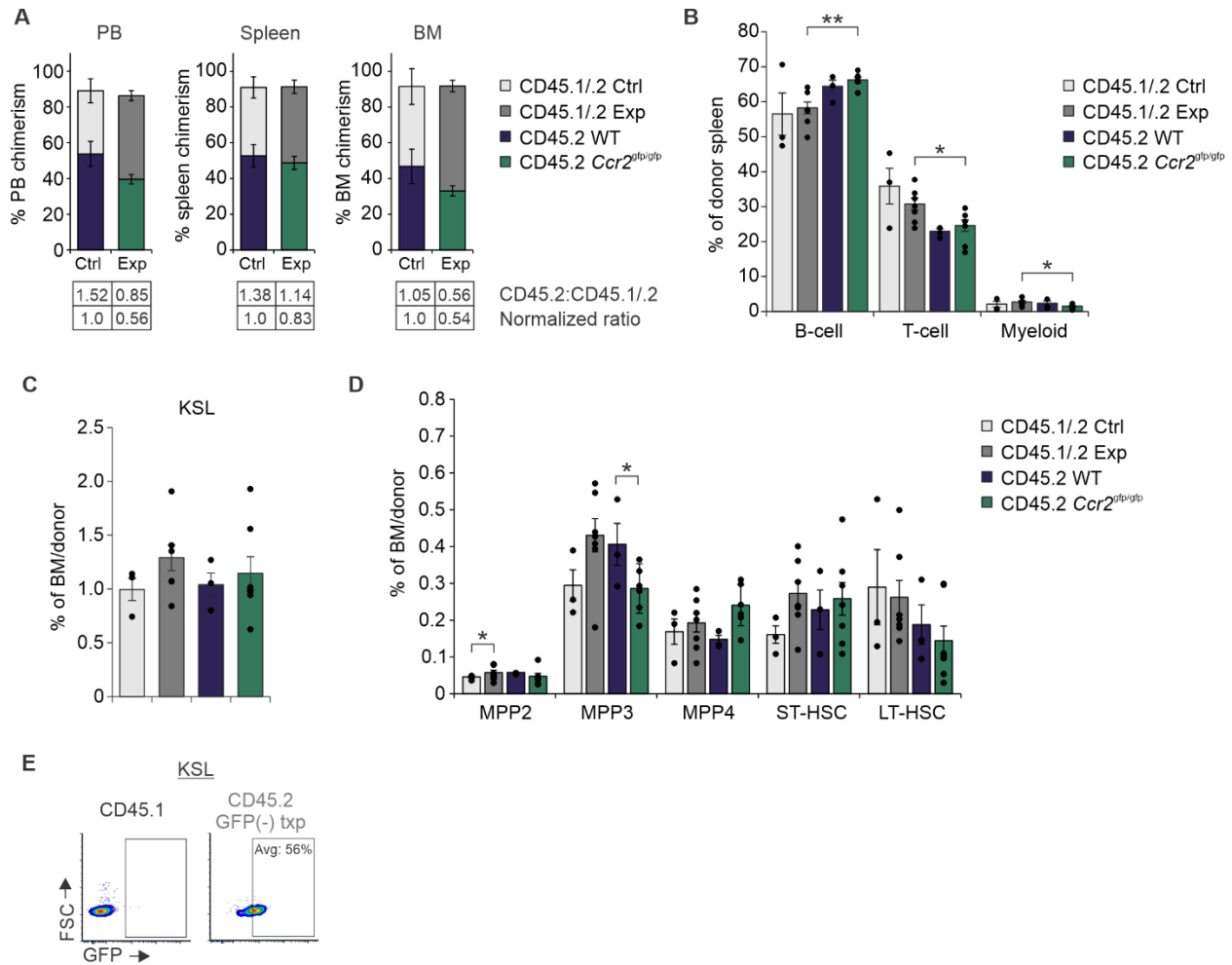


Fig. S6.

CCR2-deficient grafts show altered differentiation output. **A)** Relative total graft chimerism levels in control (Ctrl) and experimental (Exp) competitive transplantation cohorts, 12 weeks post-transplantation. **B)** Spleen lineage analysis 12 weeks post transplantation. Proportions of **C)** KSL and **D)** HSPC subpopulations in BM across donor grafts. **E)** Representative flow cytometric plot and average GFP positivity in homed KSL from starting *Ccr2*^{gfp/gfp} GFP- grafts. *, $p < 0.05$; **, $p < 0.01$.

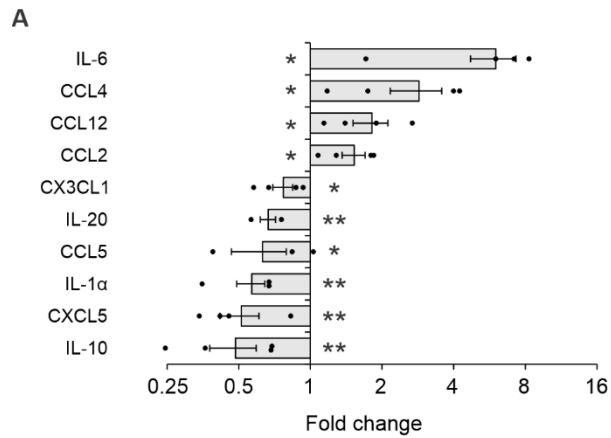


Fig. S7.

HSPC EV conditioning leads to inflammatory chemokine remodeling. A) Significantly differentially abundant cytokines or chemokines in bone marrows following HSPC EV conditioning compared to sham-injected marrows. *, $p < 0.05$; **, $p < 0.01$.

Movie S1. (separate file)

EV uptake into ECs.

Data S1. (separate file)

EV LC-MS/MS data.

Data S2. (separate file)

List of antibodies.

Data S3. (separate file)

List of primers.